PERGAMON

International Journal of Heat and Mass Transfer 44 (2001) 3553–3563

International Journal of HEAT and MASS TRANSFER

www.elsevier.com/locate/ijhmt

Approximate solutions for metallic regenerative heat exchangers

H. Klein [a,*], G. Eigenberger [b]

[a] *Linde AG, Werksgruppe Verfahrenstechnik und Anlagenbau, Dr. Carl-von-Linde-Straße 6-14, 82049 Höllriegelskreuth, Germany*
[b] *Institut für Chemische Verfahrenstechnik, Universität Stuttgart, Böblinger Straße 72, 70199 Stuttgart, Germany*

Received 18 May 1998; received in revised form 2 October 2000

Abstract

An analytical model to calculate the temperature profiles and the effectiveness of regenerative heat exchangers in counterflow is presented. It is limited to cases where the storage matrix has a small wall thickness so that no temperature variation in the matrix perpendicular to the flow direction has to be considered. This is usually the case for metallic matrices but can also be fulfilled for ceramic matrices in the form of a thin-walled monolith. Starting from a two-phase model for the gas and storage matrix an approximate solution is derived for the limiting case where the period of the hot and cold process stream becomes infinitesimally small. Using series expansions of this solution the equations to calculate the temperature profiles and the regenerator effectiveness are obtained. Contrary to already published correlations the presented analytical approach considers the heat conductivity in the storage matrix parallel to the flow direction. The range where these equations can be applied is shown by comparing the approximate solution with a numerical solution of the complete set of governing dynamic energy balance equations. The effect of important process parameters on the performance of a countercurrent regenerative heat exchanger is discussed.

1. Introduction

Regenerative heat exchangers are often used in process technology where a compact design is required. The use of a metallic storage matrix is limited to maximum temperatures of 800–1200°C, depending on the metal used, while regenerators with a ceramic storage matrix as, e.g., used for air preheating in the metallurgical industry can withstand very high temperatures [1]. Metallic regenerators feature high specific heat transfer areas which can be over 10 000 m^2 per m^3 storage volume in case of metal wire meshes. A commonly used example for metallic regenerators are rotary heat exchangers following the Ljungström principle for heat recovery applications from hot flue gases [2–5]. Rotary heat exchangers are also often used in air conditioning technology for air preheating and precooling [6,7]. Additionally to pure heat exchange, the exchange of water vapor between the two air streams can be accomplished simultaneously [8,9]. Compact metallic regenerators for cold recovery as well as for water and carbon dioxide removal had been commonly used in refrigeration technology, but due to the development of compact plate heat exchangers and sorptive drying processes they lost their original significance [2,10]. Regenerative gas cycle processes following the Stirling principle offer another application for metallic regenerators. In these processes a high thermal efficiency of the working gas cycle can only be achieved with regenerators whose effectiveness is close to 100% [11,12]. Highly efficient regenerative heat exchangers used in regenerative refrigeration cycles and heat pump processes are not only the premises for high effectiveness numbers but decisive that the principle works at all [13]. In gas turbine applications rotary regenerative heat exchangers are widely used. In order to achieve a high efficiency of the gas cycle process a careful analysis of the thermal performance of the regenerator is required [14].

* Corresponding author. Tel.: +49-89-74453732; fax: +49-89-74454945.
E-mail address: harald.klein@linde-va.de (H. Klein).

0017-9310/01/$ - see front matter
PII: S0017-9310(01)00010-2

Nomenclature

A_R	cross-sectional area of regenerator (m^2)
a_V	specific heat transfer area (m^2/m^3)
c_p	specific heat capacity gas (J/kg K)
c_s	specifcic heat capacity solid (J/kg K)
G_z	mass flux gas (kg/m^2 s)
L_R	regenerator length (m)
$\dot{m}$	mass flow rate gas (kg/s)
NTU	number of transfer units
Pe	Péclet number
Q_R	heat stored in regenerator (J)
Q_R^{ideal}	heat stored in regenerator under ideal conditions (J)
$\dot{Q}_\lambda$	heat flux via conduction (W)
$\dot{Q}_\alpha$	heat flux between gas and solid (W)
t	time (s)
Δt	length of one half-period (switching time) (s)
z	flow length coordinate (m)

Greek symbols

α	heat transfer coefficient (W/m^2 K)
ε	porosity of regenerator
Γ	ratio of solid mass to gas mass in regenerator
ζ	dimensionless flow length
η_R	regenerator effectiveness
λ_z	heat conductivity parallel to flow direction (W/m K)
λ_r	heat conductivity perpendicular to flow direction (W/m K)
ϱ	density of gas (kg/m^3)
ϱ_s	density of solid (kg/m^3)
σ	ratio of heat capacities
τ	dimensionless time

Subscripts and superscripts

g	gas
s	solid
1	half-period 1 (inlet of hot gas)
2	half-period 2 (inlet of cold gas)
in	inlet
out	outlet
$^-$	averaged over one half-period

In the past numerous calculation methods were developed to determine the temperature profile of the gas and the storage matrix in regenerative heat exchangers as well as their effectiveness. Nußelt [15] developed four analytical methods and one graphical method for the calculation of the temperature profiles where each method is based on assumptions concerning the heat conduction parallel (λ_z) and perpendicular (λ_r) to the flow direction of the gas. In a second paper Nußelt [16] developed an analytical solution for the periodic-steady state for negligible heat conduction parallel and infinite heat conduction perpendicular to flow direction (case 3 of [15]). In all cases presented by Nußelt the energy of the gas entrained in the storage matrix (compared to the energy of the solid material) is neglected at the period switches. Unless otherwise stated this has been assumed for all models cited in this paper.

Different solutions were presented for the model based on the assumption of negligible heat conduction parallel and infinite heat conduction perpendicular to flow direction ($\lambda_z = 0, \lambda_r = \infty$). Among them most are based on numerical finite difference schemes where the periodic-steady state solution is obtained from initial guesses of the temperature profiles and successive substitution [4,5,17–20]. Kays and London [21] correlated the results obtained from numerical solutions to a simple algebraic equation for the regenerator effectiveness. The time-consuming iteration scheme can be avoided using the closed solution methods being published in [22–25].

All models and solutions cited above do not take into account longitudinal heat conduction. This effect was first considered in the numerical model developed by Bahnke and Howard [26]. These results were correlated by Shah [27] to an algebraic equation for the regenerator effectiveness. New models taking into account heat conductivity parallel and perpendicular to the flow direction (two-dimensional heat conduction in the matrix) are still subject to numerical solution schemes using explicit finite-difference methods and successive substitution for obtaining periodic-steady state [28,29]. A model developed by Ren and Wang [30] considers the effect of longitudinal heat conduction as well as temperature-depended thermal properties. Furthermore, in the numerical investigation the energy of the gas entrained in the storage matrix is taken into account. This effect is small if the residence time of the gas within the matrix is small compared to the length of one period [31]. For regenerators in Stirling engines this assumption is usually not fulfilled. Models with closed analytical solutions have been developed where the dynamic behavior of the gas phase entrained in the matrix is considered [32,33]. These models take into account that part of the gas remains within the channels of the matrix from one period to the other introducing the so-called *flushing phase*. However, other assumptions such as infinite thermal capacity and zero heat conductivity parallel to the fluid flow of the storage matrix are required to obtain a closed solution of the problem.

The following table shows a summary of the models and their solution scheme for thermal regenerators cited above. It can be seen that no closed analytical solution has been presented so far taking into account the axial heat conductivity of the storage matrix. The solution developed from thermophysical basic equations presented in this paper is an approach to close this gap.

Model assumption	Finite difference solutions	Closed solutions
Short switching times		Nußelt case 1 [15]
$\lambda_z = 0,\ \lambda_r = \infty$	Lambertson [17] Willmott [18] Zafeiriou and Wurz [4] Hill and Willmott [19,20]	Nußelt case 3 [15] Hill and Willmott [22] Scaricabarozzi [23,24] Atthey [25]
$\lambda_z > 0,\ \lambda_r > 0$	Shen and Worek [28,29]	
$\lambda_z > 0,\ \lambda_r = \infty$	Bahnke and Howard [26] Shah [27]	Klein and Eigenberger (this paper)
$\lambda_z = 0,\ \lambda_r > 0$	Nußelt case 5 [15] Willmott [35]	Hausen [34]
$\lambda_z = 0,\ \lambda_r = \infty$	Ren and Wang [30]	de Monte [33]
incl. gas energy storage	Willmott and Hinchcliffe [31]	

2. Dynamic energy balances

Regenerators are structures in which the temperatures change continuously both in space and in time. The temperature change perpendicular to the main flow direction can be usually neglected if metallic regenerators or regenerators with a comparatively small wall thickness of the storage material are used. Therefore, a one-dimensional dynamic two-phase model according to Fig. 1 with energy balance equations for the flowing gas phase and for the solid matrix can sufficiently describe the relevant effects in the regenerator [36]. Axial heat conduction will be considered only in the matrix due to higher heat conductivity compared to the gas. The energy balance for the volume element shown in Fig. 1 yields the following model of the regenerator:

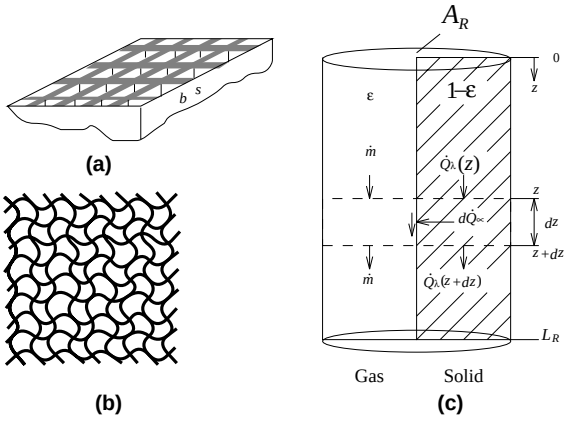

Fig. 1. Regenerator structures and control volume for the one-dimensional heterogeneous two-phase model: (a) monolithic structure, (b) wire mesh; (c) model.

$$\varepsilon\varrho c_p \frac{\partial T_g}{\partial t} = \mp G_z c_p \frac{\partial T_g}{\partial z} + \alpha a_V (T_s - T_g), \tag{1}$$

$$(1-\varepsilon)\varrho_s c_s \frac{\partial T_s}{\partial t} = \lambda_z \frac{\partial^2 T_s}{\partial z^2} - \alpha a_V (T_s - T_g). \tag{2}$$

In order to formulate boundary conditions the solid matrix is considered to be adiabatically insulated at both boundaries. The inlet temperatures are assumed to be constant for both half-periods. According to Fig. 2 the convection term is positive during the first half-period ($0 < t < \Delta t$) with gas flow from right to left. In the second half-period ($\Delta t < t < 2\Delta t$) the gas flows from left to right and the negative sign is valid. The mass flow rate is assumed to be constant and to have the same value for both half-periods which holds also for the heat capacities ("balanced regenerator", $G_{z1}c_{p1} = G_{z2}c_{p2}$). The mass flux G_z is referred to the regenerator cross-sectional area A_R.

Since the outlet temperature changes during each cycle it has to be averaged over one half-period to define

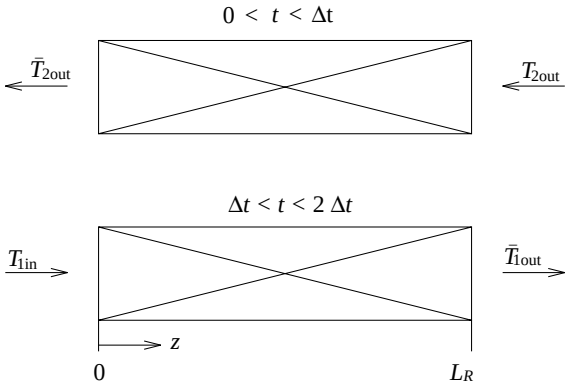

Fig. 2. Regenerator with periodic switch of flow direction.

the regenerator effectiveness (index 1 represents the inlet of hot gas at $z = 0$, index 2 the inlet of cold gas at $z = L$):

$$\eta_R = \frac{Q_R}{Q_R^{ideal}} = \frac{T_{1in} - \bar{T}_{1out}}{T_{1in} - T_{2in}} = \frac{\bar{T}_{2out} - T_{2in}}{T_{1in} - T_{2in}}. \quad (3)$$

The energy of the gas entrained in the storage matrix will be neglected compared to the energy of the solid matrix. This assumption is in accordance with most of the models published for regenerative heat exchangers [4,5,15–20]. It can be justified by comparing the time constants of the two differential equations in Eqs. (1) and (2). The volumetric heat capacity of the matrix $\varrho_s c_s$ is two to three orders of magnitude bigger than the one for the gas phase ϱc_p. Therefore, the energy balance of the gas phase can be considered as *quasi-stationary* [37,38]:

$$\mp G_z c_p \frac{\partial T_g}{\partial z} = \alpha a_V (T_s - T_g). \quad (4)$$

In this case the dynamic changes in the gas phase are neglected after switching the flow direction. The gas temperature profile jumps with each change of the flow direction, an assumption which breaks down if the cycle time approaches the residence time but holds for conventional regenerator applications such as rotary heat exchangers.

After introduction of the dimensionless variables

$$\tau = \frac{t}{2\Delta t} \quad \text{and} \quad \zeta = \frac{z}{L_R} \quad (5)$$

the following energy balances and boundary conditions result for the first half-period ($0 \leqslant \tau < 0.5$):

$$\frac{\partial T_{g2}}{\partial \zeta} = 2\mathrm{NTU}(T_s - T_{g2}), \quad (6)$$

$$\sigma\Gamma \frac{\partial T_s}{\partial \tau} = \frac{1}{Pe} \frac{\partial^2 T_s}{\partial \zeta^2} - 2\mathrm{NTU}(T_s - T_{g2}), \quad (7)$$

$$T_{g2}\big|_{\zeta=1} = T_{2in}, \quad (8)$$

$$\left.\frac{\partial T_s}{\partial \zeta}\right|_{\zeta=0} = 0, \quad (9)$$

$$\left.\frac{\partial T_s}{\partial \zeta}\right|_{\zeta=1} = 0. \quad (10)$$

The result for the second half-period ($0.5 \leqslant \tau < 1$) is

$$-\frac{\partial T_{g1}}{\partial \zeta} = 2\mathrm{NTU}(T_s - T_{g1}), \quad (11)$$

$$\sigma\Gamma \frac{\partial T_s}{\partial \tau} = \frac{1}{Pe} \frac{\partial^2 T_s}{\partial \zeta^2} - 2\mathrm{NTU}(T_s - T_{g1}), \quad (12)$$

$$T_{g1}\big|_{\zeta=0} = T_{1in}, \quad (13)$$

$$\left.\frac{\partial T_s}{\partial \zeta}\right|_{\zeta=0} = 0, \quad (14)$$

$$\left.\frac{\partial T_s}{\partial \zeta}\right|_{\zeta=1} = 0. \quad (15)$$

The so-called *number of transfer units*, NTU, serves as a measure for the quality of the heat transfer between the gas and the matrix and is defined as follows:

$$\mathrm{NTU} = \frac{\alpha a_V L_R}{2 G_z c_p}. \quad (16)$$

The relation of energy transport through convective flow to heat conduction is described by the *Péclet number*:

$$Pe = \frac{G_z c_p L_R}{\lambda_z}. \quad (17)$$

Additionally, the following parameters are important for the dynamic behavior of the regenerator: [1]

$$\sigma = \frac{c_s}{c_p}, \quad (18)$$

$$\Gamma = \frac{(1-\varepsilon)\varrho_s L_R}{2\Delta t G_z}. \quad (19)$$

The product $\sigma\Gamma$ can be interpreted as the ratio of heat storage capacity of the solid matrix to that of the flowing gas during one complete period.

3. Limiting case of fast switching

Often the solution of the countercurrent recuperative heat exchanger is used to describe in a simplified way the behavior of a regenerator with short switching times [15,37]. However, fast switching of the streams is only an incomplete condition for the useability of the countercurrent recuperator solution. More characteristic is the product $\sigma\Gamma$. This section will give a derivation of the fast switching solution starting from the dynamic differential equations of the regenerator.

The solid energy balances, Eqs. (7) and (12), are integrated over one complete cycle

$$\begin{aligned}\sigma\Gamma \int_0^1 \frac{\partial T_s}{\partial \tau}\,\mathrm{d}\tau &= \sigma\Gamma[T_s(\tau=1) - T_s(\tau=0)] \\ &= \frac{1}{Pe}\int_0^1 \frac{\partial^2 T_s}{\partial \zeta^2}\,\mathrm{d}\tau - 2\mathrm{NTU} \\ &\quad \times \int_0^{0.5} (T_s - T_{g2})\,\mathrm{d}\tau - 2\mathrm{NTU} \\ &\quad \times \int_{0.5}^1 (T_s - T_{g1})\,\mathrm{d}\tau. \end{aligned} \quad (20)$$

In the cyclic-stationary state the solid temperature at the end of the cycle $T_s(\tau = 1)$ is equal to that at the beginning $T_s(\tau = 0)$ such that

[1] Hausen [2,13,34] used in his investigations the reduced period length $\Pi = \mathrm{NTU}/(2\sigma\Gamma)$ and the reduced regenerator length $\Lambda = 2\mathrm{NTU}$.

$$0 = \frac{1}{Pe}\frac{\partial^2}{\partial\zeta^2}\int_0^1 T_s\,d\tau - 2\mathrm{NTU}\int_0^{0.5}(T_s - T_{g2})\,d\tau - 2\mathrm{NTU}\int_{0.5}^1 (T_s - T_{g1})\,d\tau. \quad (21)$$

The following Taylor-series expansion will be used to evaluate the integrals

$$T_s(\tau) = T_s(\tau = 0) + \left.\frac{\partial T_s}{\partial\tau}\right|_{\tau=0}\tau + \mathcal{O}(\tau^2). \quad (22)$$

From the dimensionless energy balance for the solid matrix

$$\frac{\partial T_s}{\partial\tau} = \frac{1}{Pe\,\sigma\Gamma}\frac{\partial^2 T_s}{\partial\zeta^2} - \frac{2\mathrm{NTU}}{\sigma\Gamma}(T_s - T_g) \quad (23)$$

it follows for the limiting case $\sigma\Gamma \to \infty$

$$\lim_{\sigma\Gamma\to\infty}\frac{\partial T_s}{\partial\tau} = 0 \quad (24)$$

and therefore

$$T_s(\tau) = T_s(\tau = 0) \neq f(\tau). \quad (25)$$

Since the gas phase is considered in quasi-steady state it follows:

$$T_{g1}(\tau) = T_{g1}(\tau = 0) \neq f(\tau), \quad (26)$$

$$T_{g2}(\tau) = T_{g2}(\tau = 0) \neq f(\tau), \quad (27)$$

i.e., the temperature of the solid and the gas phase are independent of the time τ. Therefore Eq. (21) can be written as

$$0 = \frac{1}{Pe}\frac{\partial^2 T_s}{\partial\zeta^2} - \mathrm{NTU}(T_s - T_{g2}) - \mathrm{NTU}(T_s - T_{g1}). \quad (28)$$

This equation is identical with the stationary energy balance of the solid in a countercurrent recuperative heat exchanger with equal flow rates where axial heat conduction is considered. This equation can also be obtained with the assumption of infinitesimally fast switching of the flow direction [37]. The above derivation however shows that the correct criterion for limiting behavior is a very high value of the product

$$\sigma\Gamma = \frac{c_s}{c_p}\frac{(1-\varepsilon)\varrho_s L_R}{2\Delta t G_z}. \quad (29)$$

This is achieved via [39]

- short switching time Δt,
- low mass flux G_z,
- high regenerator length L_R,
- solids with high density ϱ_s,
- solids with high specific heat capacity c_s and
- gases with low specific heat capacity c_p.

The following system of *ordinary differential equations* is obtained as an approximation for a regenerative heat exchanger with axial heat conduction and high values of $\sigma\Gamma$

$$\frac{1}{Pe}\frac{d^2 T_s}{d\zeta^2} = \mathrm{NTU}(T_s - T_{g2}) + \mathrm{NTU}(T_s - T_{g1}), \quad (30)$$

$$\frac{dT_{g1}}{d\zeta} = 2\mathrm{NTU}(T_s - T_{g1}), \quad (31)$$

$$-\frac{dT_{g2}}{d\zeta} = 2\mathrm{NTU}(T_s - T_{g2}). \quad (32)$$

The boundary conditions are

$$T_{g1}\big|_{\zeta=0} = T_{1in}, \quad (33)$$

$$T_{g2}\big|_{\zeta=1} = T_{2in}, \quad (34)$$

$$\left.\frac{dT_s}{d\zeta}\right|_{\zeta=0} = 0, \quad (35)$$

$$\left.\frac{dT_s}{d\zeta}\right|_{\zeta=1} = 0. \quad (36)$$

An analytical solution of this boundary value problem was obtained using the computer algebra system MAPLE [40]. The resulting spatial profiles along the regenerator length of the gas and solid temperatures depend on the parameters NTU and *Pe* as well as on the inlet temperatures. The limiting solution is valid for regenerators with $\sigma\Gamma \to \infty$ and will be called the *zero-order solution*. With the abbreviations $k_1 = \sqrt{2\mathrm{NTU}}\sqrt{2\mathrm{NTU} + Pe}$ and $k_2 = \sqrt{2\mathrm{NTU}}/\sqrt{2\mathrm{NTU} + Pe}$ the solution has the following form:

$$T_s^0(\zeta) = \frac{(T_{1in} + T_{2in})\left(\frac{e^{k_1}-1}{e^{k_1}+1}k_2 + 1 + \frac{Pe}{2\mathrm{NTU}}\right) + T_{1in}Pe}{2 + Pe + \frac{Pe}{\mathrm{NTU}} + 2k_2\frac{e^{k_1}-1}{e^{k_1}+1}} + \frac{(T_{2in} - T_{1in})\left(Pe\zeta + \frac{Pe}{2\mathrm{NTU}}k_2\frac{e^{k_1(1-\zeta)} - e^{k_1\zeta}}{e^{k_1}+1}\right)}{2 + Pe + \frac{Pe}{\mathrm{NTU}} + 2k_2\frac{e^{k_1}-1}{e^{k_1}+1}}, \quad (37)$$

$$T_{g1}^0(\zeta) = \frac{(T_{1in} + T_{2in})\left(\frac{e^{k_1}-1}{e^{k_1}+1}k_2 + 1\right) + Pe\left(T_{1in} + \frac{T_{1in}}{\mathrm{NTU}}\right)}{2 + Pe + \frac{Pe}{\mathrm{NTU}} + 2k_2\frac{e^{k_1}-1}{e^{k_1}+1}} + \frac{(T_{2in} - T_{1in})\left(Pe\zeta - \frac{e^{k_1(1-\zeta)} + e^{k_1\zeta}}{e^{k_1}+1} - k_2\frac{e^{k_1(1-\zeta)} - e^{k_1\zeta}}{e^{k_1}+1}\right)}{2 + Pe + \frac{Pe}{\mathrm{NTU}} + 2k_2\frac{e^{k_1}-1}{e^{k_1}+1}}, \quad (38)$$

$$T_{g2}^0(\zeta) = \frac{(T_{1in} + T_{2in})\left(\frac{e^{k_1}-1}{e^{k_1}+1}k_2 + 1\right) + Pe\left(T_{1in} + \frac{T_{2in}}{\mathrm{NTU}}\right)}{2 + Pe + \frac{Pe}{\mathrm{NTU}} + 2k_2\frac{e^{k_1}-1}{e^{k_1}+1}} + \frac{(T_{2in} - T_{1in})\left(Pe\zeta + \frac{e^{k_1(1-\zeta)} + e^{k_1\zeta}}{e^{k_1}+1} - k_2\frac{e^{k_1(1-\zeta)} - e^{k_1\zeta}}{e^{k_1}+1}\right)}{2 + Pe + \frac{Pe}{\mathrm{NTU}} + 2k_2\frac{e^{k_1}-1}{e^{k_1}+1}}. \quad (39)$$

The zero-order solution for the temperature profiles is shown in Fig. 3. The solid temperature profile T_s^0 is

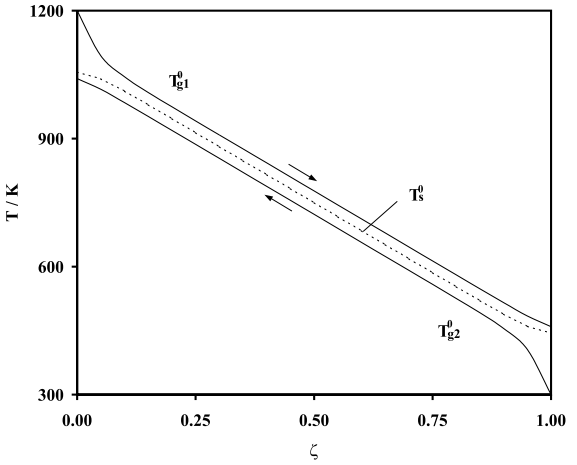

Fig. 3. Zero-order solution of the regenerator or countercurrent heat exchanger solution for $T_{1in} = 1200$ K, $T_{2in} = 300$ K and NTU = 11.95, $Pe = 12.59$.

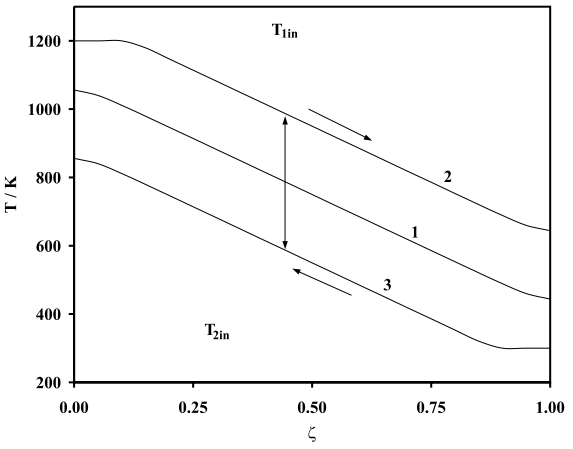

Fig. 4. Temperature profiles in the regenerator.

significantly flattened compared to the connecting line between the two inlet temperatures ($T_{1in} = 1200$ K, $T_{2in} = 300$ K). This is due to the heat conductivity in the storage material ($Pe = 12.59$). Starting from the respective inlet temperature, the gas-phase temperature T^0_{g1} or T^0_{g2} approaches the solid temperature for both half-periods. The remaining difference at the outlet is due to the limited heat transfer rate between the solid and the gas phase (NTU = 11.95).

The quality of the heat exchanger is described through the regenerator effectiveness η_R according to Eq. (3). With the above equations the zero-order solution for the effectiveness is

$$\eta^0_R = \frac{Pe + 2k_2((e^{k_1} - 1)/(e^{k_1} + 1))}{2 + Pe + (Pe/\mathrm{NTU}) + 2k_2((e^{k_1} - 1)/(e^{k_1} + 1))}. \tag{40}$$

This relation is independent of the inlet conditions. Eq. (40) changes for $Pe \to \infty$ to the special case of the countercurrent heat exchanger without axial heat conduction [21]

$$\eta^0_R = \frac{\mathrm{NTU}}{1 + \mathrm{NTU}}. \tag{41}$$

4. Approximation of the regenerator via a series expansion

The above solution is only valid in the limit of $\sigma\Gamma \to \infty$. A more general approximative solution of the balance equations can be obtained as follows. This approximation is hereafter referred to as *first-order solution*.

Before going through the mathematical derivation a more qualitative interpretation of the derived first-order solution will be given. In the periodic-steady state the solution profiles oscillate around the profiles of Fig. 3. This oscillation is shown in Fig. 4 for the case of the solid temperature. The solid temperature profile moves from position 2 to position 3 during flow of cold gas from the right to the left and from 3 back to 2 during the flow of hot gas from the left to the right. The zero-order solution, profile 1, will thus be a mean value profile between profiles 2 and 3 with the following restriction: since the solid temperature at the left-hand side ($\zeta = 0$) can never exceed the feed gas temperature T_{1in} and at the right-hand side ($\zeta = 1$) can never fall below T_{2in} profile 2 is bounded by T_{1in} and profile 3 by T_{2in}. The assumption of the depicted vertical shift of profile 1 (within the limits of T_{1in} and T_{2in}) has the advantage that the boundary conditions of the intermediate profiles remain physically correct.

4.1. Calculation of the temperature profiles

The energy balance for the solid as given by Eq. (7) or (12) is

$$\frac{\partial T_s}{\partial \tau} = \mu_1\mu_2 \frac{\partial^2 T_s}{\partial \zeta^2} - 2\mathrm{NTU}\mu_2(T_s - T_g), \tag{42}$$

where the following abbreviations are used

$$\mu_1 = \frac{1}{Pe} \quad \text{and} \quad \mu_2 = \frac{1}{\sigma\Gamma}. \tag{43}$$

The zero-order solution for Eq. (42) was derived under the assumption $\mu_2 = 0$. It contains the full dependence on the heat transfer parameter NTU and the axial conductivity μ_1. In order to derive a first-order solution T^1_s we use a Taylor series expansion of T_s for the additional parameter μ_2 around $T^0_s = T_s(\mu_1 = 0, \mu_2 = 0)$

$$T_s^1 = T_s^0 + \left.\frac{\partial T_s}{\partial \mu_2}\right|_{\substack{\mu_1=0\\ \mu_2=0}} \mu_2 + \frac{1}{2}\left.\frac{\partial^2 T_s}{\partial \mu_2^2}\right|_{\substack{\mu_1=0\\ \mu_2=0}} \mu_2^2 + \cdots \tag{44}$$

With the abbreviation

$$\psi = \left.\frac{\partial T_s}{\partial \mu_2}\right|_{\substack{\mu_1=0\\ \mu_2=0}} + \frac{1}{2}\left.\frac{\partial^2 T_s}{\partial \mu_2^2}\right|_{\substack{\mu_1=0\\ \mu_2=0}} \mu_2 + \cdots \tag{45}$$

it follows

$$T_s^1 = T_s^0 + \mu_2 \psi. \tag{46}$$

Since T_s^0 is the time independent stationary solution, it disappears after derivating with respect to the dimensionless time τ and Eq. (46) gives

$$\frac{\partial T_s^1}{\partial \tau} = \mu_2 \frac{\partial \psi}{\partial \tau}. \tag{47}$$

The solid energy balance, Eq. (42), can be written for $\mu_1 = 0$ (neglecting axial conduction) as

$$\frac{\partial T_s}{\partial \tau} = -2\mathrm{NTU}\mu_2(T_s - T_g) = -2\mathrm{NTU}\mu_2\left[T_s^0(\mu_1 = 0) - T_g^0(\mu_1 = 0)\right]. \tag{48}$$

This means that the solid temperature profile moves upwards or downwards as in Fig. 4, if the temperature difference $(T_s - T_g)$ is positive or negative. Due to the quasi-stationarity of the gas phase the difference between solid and gas temperature is constant even for transient profiles. Therefore, the following ordinary differential equation for ψ can be obtained from Eq. (47)

$$\frac{\mathrm{d}\psi}{\mathrm{d}\tau} = -2\mathrm{NTU}\left[T_s^0(\mu_1 = 0) - T_g^0(\mu_1 = 0)\right]. \tag{49}$$

This equation can be integrated directly if the following case distinction is made:

$0 \leqslant \tau < 0.5$:

$$\psi = -2\mathrm{NTU}\left[T_s^0(\mu_1 = 0) - T_{g2}^0(\mu_1 = 0)\right]\tau + C_2, \tag{50}$$

$0.5 \leqslant \tau < 1$:

$$\psi = -2\mathrm{NTU}\left[T_s^0(\mu_1 = 0) - T_{g1}^0(\mu_1 = 0)\right]\tau + C_1. \tag{51}$$

The solution profiles for $\mu_1 = 0$ are required to calculate the difference between solid and gas temperatures. They are derived from Eq. (37) to (39) for the limiting case $Pe \to \infty$:

$$T_s^0(\mu_1 = 0) = \frac{\mathrm{NTU}}{1 + \mathrm{NTU}}\left[\frac{T_{1\mathrm{in}} + T_{2\mathrm{in}}}{2\mathrm{NTU}} + T_{1\mathrm{in}}(1 - \zeta) + T_{2\mathrm{in}}\zeta\right], \tag{52}$$

$$T_{g1}^0(\mu_1 = 0) = T_{1\mathrm{in}} - \frac{\mathrm{NTU}}{1 + \mathrm{NTU}}(T_{1\mathrm{in}} - T_{2\mathrm{in}})\zeta, \tag{53}$$

$$T_{g2}^0(\mu_1 = 0) = T_{2\mathrm{in}} + \frac{\mathrm{NTU}}{1 + \mathrm{NTU}}(T_{1\mathrm{in}} - T_{2\mathrm{in}})(\zeta - 1). \tag{54}$$

After inserting Eqs. (50)–(54) into Eq. (46), the following relations for the transient change of the solid temperature are obtained:

$0 \leqslant \tau < 0.5$:

$$T_s^1 = T_s^0 - \frac{\mathrm{NTU}}{1 + \mathrm{NTU}}(T_{1\mathrm{in}} - T_{2\mathrm{in}})\frac{\tau - 0.25}{\sigma\Gamma}, \tag{55}$$

$0.5 \leqslant \tau < 1$:

$$T_s^1 = T_s^0 - \frac{\mathrm{NTU}}{1 + \mathrm{NTU}}(T_{1\mathrm{in}} - T_{2\mathrm{in}})\frac{0.75 - \tau}{\sigma\Gamma}. \tag{56}$$

As a condition to determine C_1 and C_2 from Eqs. (50) and (51) it shall be assumed that the temperature profile in the middle of each half-period ($\tau = 0.25$ and $\tau = 0.75$) is the same as that of the zero-order solution T_s^0, Eq. (37). This has been labeled profile 1 in Fig. 4. A period now starts from profile 1 and a symmetric shifting around this profile results.

The gas temperature follows the solid temperature such that the result can be taken directly from Eqs. (55) and (56):

$0 \leqslant \tau < 0.5$:

$$T_g^1 = T_{g2}^0 - \frac{\mathrm{NTU}}{1 + \mathrm{NTU}}(T_{1\mathrm{in}} - T_{2\mathrm{in}})\frac{\tau - 0.25}{\sigma\Gamma}, \tag{57}$$

$0.5 \leqslant \tau < 1$:

$$T_g^1 = T_{g1}^0 - \frac{\mathrm{NTU}}{1 + \mathrm{NTU}}(T_{1\mathrm{in}} - T_{2\mathrm{in}})\frac{0.75 - \tau}{\sigma\Gamma}. \tag{58}$$

Since any changes of the profile shape are neglected, solid and gas temperatures can be calculated which lie above the hot inlet and below the cold inlet temperature. In these cases the temperature has to be set equal to the respective inlet temperature. This will be shown in the following section.

4.2. Calculation of the regenerator effectiveness

In order to calculate the regenerator effectiveness via Eq. (3) the outlet temperatures can be calculated with Eq. (57) or Eq. (58) and then be integrated over the respective half-period. Considering half-period 2 (cold inlet at $\zeta = 1$) yields

$$T_{g2}^1(\zeta = 0) = T_{g2}^0(\zeta = 0) - \frac{\mathrm{NTU}}{1 + \mathrm{NTU}}(T_{1\mathrm{in}} - T_{2\mathrm{in}})\frac{\tau - 0.25}{\sigma\Gamma}. \tag{59}$$

As mentioned above, a temperature above the inlet temperature $T_{1\mathrm{in}}$ might follow from this relation due to the neglection of the form changes. In this case it is assumed that

$$T_{g2}^1(\zeta = 0) = T_{1\mathrm{in}}. \tag{60}$$

The time τ^* until Eq. (59) is valid follows from the relation

$$T^0_{g2}(\zeta=0)-\frac{\mathrm{NTU}}{1+\mathrm{NTU}}(T_{1in}-T_{2in})\frac{\tau^*-0.25}{\sigma\Gamma}=T_{1in}. \tag{61}$$

Resolved for τ^* this yields

$$\tau^*=\max\left[0,0.25-\frac{T_{1in}-T^0_{g2}(\zeta=0)}{T_{1in}-T_{2in}}\frac{1+\mathrm{NTU}}{\mathrm{NTU}}\sigma\Gamma\right]. \tag{62}$$

Therefore, the outlet temperature is

$$\tau<\tau^*: T^1_{g2}(\zeta=0)=T_{1in}, \tag{63}$$

$$\tau\geqslant\tau^*:$$

$$T^1_{g2}(\zeta=0)=T^0_{g2}(\zeta=0)-\frac{\mathrm{NTU}}{1+\mathrm{NTU}}(T_{1in}-T_{2in})\frac{\tau-0.25}{\sigma\Gamma}. \tag{64}$$

The average outlet temperature for the cold half-period results from the integration

$$\bar{T}^1_{g2}(\zeta=0)=\frac{1}{0.5}\int_0^{0.5}T^1_{g2}(\zeta=0)\,\mathrm{d}\tau. \tag{65}$$

The integral has to be split as follows:

$$\int_0^{0.5}T^1_{g2}(\zeta=0)\,\mathrm{d}\tau=\int_0^{\tau^*}T_{1in}\,\mathrm{d}\tau+\int_{\tau^*}^{0.5}\left[T^0_{g2}(\zeta=0)-\frac{\mathrm{NTU}}{1+\mathrm{NTU}}(T_{1in}-T_{2in})\frac{\tau-0.25}{\sigma\Gamma}\right]\mathrm{d}\tau. \tag{66}$$

After evaluating the individual parts it follows:

$$\bar{T}^1_{g2}(\zeta=0)=T^0_{g2}(\zeta=0)+\tau^*\left[2T_{1in}-2T^0_{g2}(\zeta=0)+\frac{\mathrm{NTU}}{1+\mathrm{NTU}}\frac{\tau^*-0.25}{\sigma\Gamma}(T_{1in}-T_{2in})\right]. \tag{67}$$

With the definition in Eq. (3) the final result for the regenerator effectiveness is

$$\eta^1_{Reg}=\eta^0_{Reg}-\tau^*\left[\frac{\mathrm{NTU}}{1+\mathrm{NTU}}\frac{0.5-\tau^*}{\sigma\Gamma}-2\frac{T_{1in}-T^0_{g2}(\zeta=0)}{T_{1in}-T_{2in}}\right], \tag{68}$$

where $T^0_{g2}(\zeta=0)$ is obtained from Eq. (58) and τ^* is calculated from Eq. (62).

In cases where the outlet temperature $T_{g2}(\zeta=0)$ moves around the value of the stationary countercurrent solution without reaching the hot inlet temperature, the effectiveness from the first-order solution is equal to the effectiveness from the zero-order solution. The regenerator effectiveness decreases when the parameter $\sigma\Gamma$ decreases, e.g., due to a higher switching time Δt, such that τ^* in Eq. (62) is above zero.

The transient change of the temperature profiles for solid and gas phase in the regenerator as well as the effectiveness can now be approximately described. The validity of this approximation can only be checked via comparison with the solution of the complete dynamic simulation model in Eqs. (1) and (2). This comparison is presented in Section 4.4. But first it has to be discussed how fine the complete dynamic model has to be discretized for its accurate numerical solution.

4.3. The required grid for an accurate regenerator in the limit of countercurrent heat exchange

In the complete dynamic two-phase model of the regenerator the spatial domain was discretisized in Eqs. (1) and (2) using the finite volume method [41]. The resulting ordinary differential equation system could then be numerically solved with the integrator LIMEX [42]. It turned out that the regenerator efficiencies

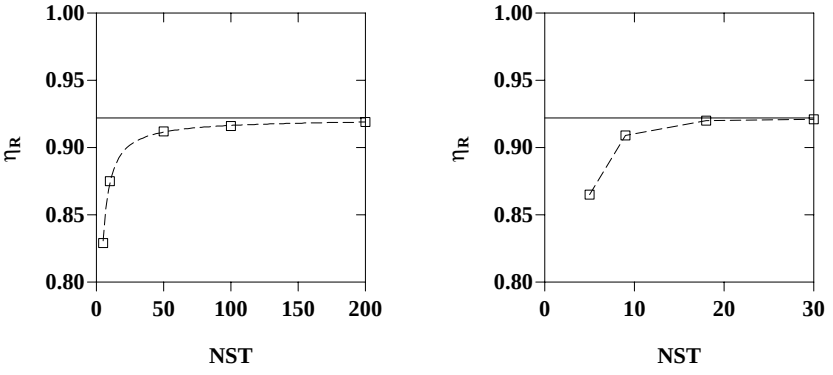

Fig. 5. Regenerator effectiveness η_R as a function of the selected number of grid points NST calculated via dynamic simulation (––) and analytical zero-order solution (—) for NTU = 11.95, $Pe\to\infty$, $\sigma\Gamma=12.31$; left: equidistant distribution, right: refined grid at the boundaries.

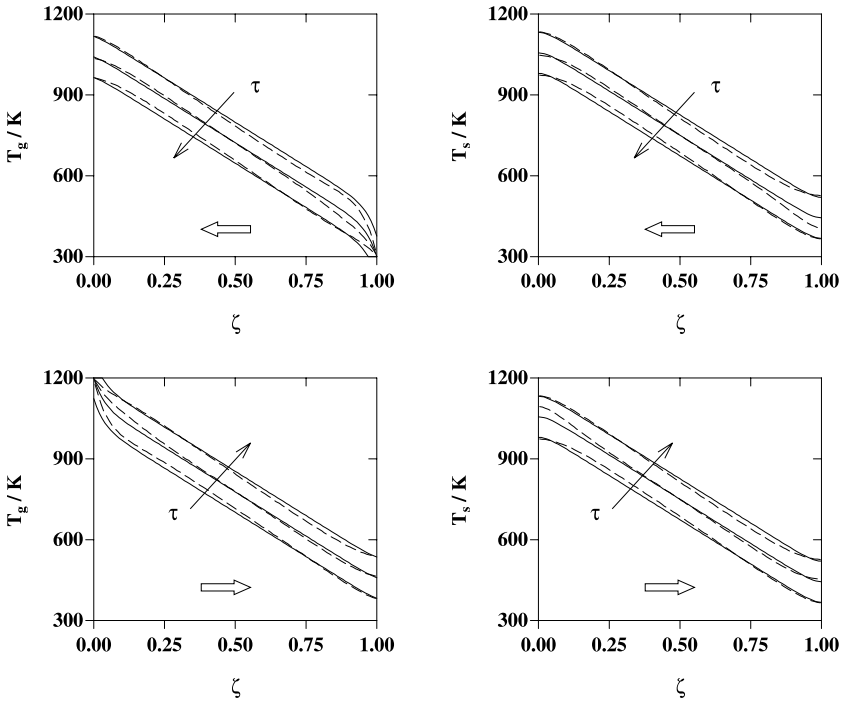

Fig. 6. Temperature profiles in the regenerator using the dynamic simulation model (––) and the approximated regenerator model (—) for $T_{1in} = 1200$ K, $T_{2in} = 300$ K and NTU = 11.95, $Pe = 12.59$, $\sigma\Gamma = 2.73$; left: gas phase, right: solid matrix; upper: half-period 2, lower: half-period 1; ⇐: flow direction.

obtained changed with the selected number of grid points. In Section 3 it was shown that a periodic regenerator will be described by the model of a countercurrent heat exchanger in the limit of large $\sigma\Gamma$ and an analytical solution was presented for this case. This solution can now be used in comparison with the numerical solution to determine the required computation grid.

Fig. 5 shows the regenerator effectiveness calculated via simulation as a function of the number NST of grid points used. The grid in the left diagram is equidistant whereas in the right diagram the grid points increase exponentially towards both boundaries (70 coarse grid points, resp. 15 fine grid points at the boundaries). The continuous line shows the analytical solution of the countercurrent recuperator which coincides with the exact solution of the regenerator due to the high value of $\sigma\Gamma$ assumed. With an equidistant grid distribution reasonable agreement is only achieved with a high number of grid points while refining the grid at the boundaries approximates the exact solution very well already at a small number of grid points.

4.4. Validation of the proposed approximated regenerator model

Fig. 6 shows a comparison of the temperature profiles obtained by simulation and with the approximated model. As shown above, the first half-period in the cyclic-stationary state is characterized by the inlet of cold gas at the right boundary ($T_{2in} = 300$ K). The gas cools the solid matrix and the gas profile follows that of the solid phase. The flow direction changes during the second half-period and hot gas ($T_{1in} = 1200$ K) enters at the left boundary. Now the solid matrix is heated up again.

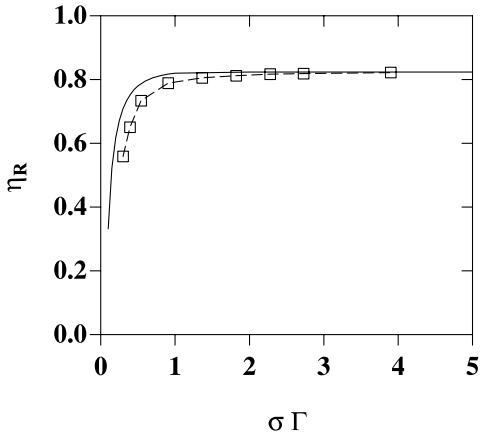

Fig. 7. Regenerator effectiveness η_R using the dynamic simulation model (––) and the approximated regenerator model (—) for NTU = 11.95, $Pe = 12.59$.

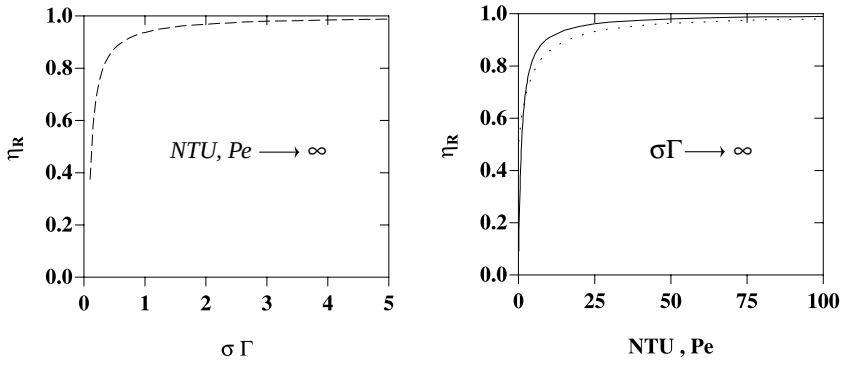

Fig. 8. Regenerator effectiveness η_R as a function of left: $\sigma\Gamma$ (––); right: NTU (—) and Pe (···).

The comparison between simulation and the approximate model shows that some differences occur in the profile shape. Important is that the reduced model shows almost exactly the correct gas outlet temperatures at each time such that the regenerator effectiveness can be estimated very well. Fig. 7 shows that this is especially valid for higher values of $\sigma\Gamma$. Regenerative heat exchangers are often used in process technology under conditions where the temperature profiles move as little as possible. This is exactly the range where the reduced model describes the regenerator behavior with high accuracy, but also the failure of the regenerator at low values of $\sigma\Gamma$ is well represented.

4.5. Effect of parameters on regenerator effectiveness

The calculation method presented above allows the determination of the regenerator effectiveness η_R depending on the parameters $\sigma\Gamma$, NTU und Pe. With ideal conditions for the heat transfer and no axial heat conduction (NTU, $Pe \to \infty$) an almost ideal regenerator behavior can be already achieved at a value of $\sigma\Gamma = 5$, as shown in Fig. 8 on the left-hand side. Values of $\approx$100 for the parameters NTU and Pe have to be reached for a comparably high effectiveness at ideal heat storage characteristics ($\sigma\Gamma \to \infty$). Therefore, NTU and Pe are the key parameters to develop highly efficient regenerators.

5. Conclusion

The presented model and its analytical solution allow for an simplified calculation of the temperature profiles in regenerative heat exchangers and for a good approximation of regenerator effectiveness. In the technically relevant region the approximative solution fits to the numerical solution of the one-dimensional dynamic two-phase model. Especially the calculation of the gas outlet temperatures and therefore the effectiveness as a function of the parameters NTU, Pe and $\sigma\Gamma$ are very well approximated. A value of $\sigma\Gamma = 5$ is sufficient for efficiencies higher than 98% if optimal conditions for heat transfer and heat conduction are chosen. In case of ideal heat storage characteristics a value of $\approx$100 has to be reached for the parameters NTU and Pe in order to obtain efficiencies close to one.

References

[1] R. Donald, Simulation and Control of Blast Furnace Hot Blast Stoves, Institution of Engineers, Australia, National Conferenece Publication, 1992.
[2] H. Hausen, in: Wärmeübertragung im Gegenstrom, Gleichstrom und Kreuzstrom, Springer, Berlin, 1970.
[3] H. Martin, in: Wärmeübertrager, Georg Thieme Verlag, Stuttgart, 1988.
[4] E. Zafeiriou, D. Wurz, Numerische Simulation der Wärmeübertragungsvorgänge in rotierenden Regeneratoren, VGB Kraftwerkstechnik, 76 (1996) 463–470.
[5] H. Kreis, D. Mihailowitsch, Einsatz von Regeneratoren in Anlagen zur Rauchgasreinugung, Linde Berichte auf Wissenschaft und Technik, 59, 1986.
[6] ASHREA, Handbook of Fundamentals, American Society of Heating, Refrigeration and Air Conditioning Engineers, New York, 1985.
[7] J.W. Mitchell, in: Energy Engineering, Wiley, New York, 1983.
[8] J. van Leersum, Heat and mass transfer in regenerators, Ph.D. thesis, Monash University, Australia, 1975.
[9] R. Vauth, Wärme- und Stoffaustausch in regenerativen Wärmetauschern mit rotierenden nicht adsorbierenden Speichermassen, Forsch. Ber. D. Kälte- und Klimatechnischen Vereins Nr. 1, Stuttgart, 1979.
[10] Ullmann's Encyclopedia of Industrial Chemistry, Vol. A18, VCH, 1991.
[11] A.J. Organ, in: Thermodynamics and Gas Dynamics of the Stirling Cycle Machine, Cambridge University Press, New York, 1992.
[12] G. Walker, in: Stirling Engines, Clarendon Press, Oxford, 1980.
[13] C.M. Hargreaves, in: The Philips Stirling Engine, Elsevier, Amsterdam, 1991.

[14] A.J. Organ, Analysis of the gas turbine rotary regenerator, Proc. Instn. Mech. Eng., J. Automobile Eng. 211 (1997) 97–111.
[15] W. Nußelt, Die Theorie des Winderhitzers, VDI-Zeitung, 71 (1927) 85–91.
[16] W. Nußelt, Der Beharrungszustand im Winderhitzer, VDI-Zeitung, 72 (1928) 1052–1054.
[17] T.J. Lambertson, Performance factors of a periodic flow heat exchanger, ASME Trans. 80 (1958) 586–592.
[18] A.J. Willmott, Digital computer simulation of a thermal regenerator, Int. J. Heat Mass Transfer 7 (1964) 1291–1302.
[19] A. Hill, A.J. Willmott, A robust method for regenerative heat exchanger calculations, Int. J. Heat Mass Transfer 30 (1987) 241–249.
[20] A. Hill, A.J. Willmott, Accurate and rapid thermal regenerator calculations, Int. J. Heat Mass Transfer 32 (1989) 465–476.
[21] A.L. Kays, W.M. London, in: Compact Heat Exchangers, McGraw-Hill, New York, 1984.
[22] A. Hill, A.J. Willmott, Modelling the temperature dependence of thermophysical properties in a closed method for regenerative heat exchanger simulations, Proc. Instn. Mech. Eng. 202 (1991) 195–206.
[23] R. Scaricabarozzi, Simple particular solutions and speed calculation of regenerators, Heat Recovery Syst. CHP 9 (1989) 421–432.
[24] R. Scaricabarozzi, Une méthod numériqué non itérative pour la détermination du régime fonctionnement périodique des régénérateurs, Int. J. Heat Mass Transfer 32 (1989) 409–414.
[25] D.R. Atthey, An approximate thermal analysis for a regenerative heat exchanger, Int. J. Heat Mass Transfer 31 (1988) 1431–1441.
[26] G.D. Bahnke, C.P. Howard, The effect of longitudinal heat conduction on periodic flow heat exchanger performance, ASME J. Eng. Power 86 (1964) 105–120.
[27] R.K. Shah, A correlation for longitudinal heat conduction effects in periodic flow heat exchanger, ASME J. Eng. Power 97 (1975) 453–454.
[28] C.M. Shen, W.M. Worek, A correlation for the heat conduction effects in counterflow rotary regenerative heat exchangers, ASME J. Energy Resour. Technol. 115 (1993) 287–290.
[29] C.M. Shen, W.M. Worek, The effect of wall conduction on the performance of regenerative heat exchangers, Energy 17 (1992) 1199–1213.
[30] Z. Ren, S. Wang, A theoretical and experimental investigation of heat transfer performance of rotary regenerative heat exchangers, Heat Transfer Science and Technology, Conference Article, Hemisphere, Washington, DC, 1987.
[31] A.J. Willmott, C. Hinchcliffe, The effect of gas heat storage regenerator calculations, Int. J. Heat Mass Transfer 19 (1976) 821–826.
[32] A.J. Organ, The wire mesh regenerator of the Stirling cycle machine, Int. J. Heat Mass Transfer 37 (1994) 2525–2534.
[33] F. de Monte, Cyclic steady thermal response of rapidly switched fixed-bed heat regenerators in counterflow, Int. J. Heat Mass Transfer 42 (1999) 2591–2604.
[34] Verein Deutscher Ingenieure, Hrsg. VDI-Wärmeatlas – Berechnungsblätter für den Wärmeübergang, VDI-Verlag, Düsseldorf, 1991.
[35] A.J. Willmott, The regenerative heat exchanger computer representation, Int. J. Heat Mass Transfer 12 (1969) 997–1013.
[36] G. Spiga, M. Spiga, A rigorous solution to a heat transfer two phase model in porous media and packed beds, Int. J. Heat Mass Transfer 24 (1981) 355–364.
[37] U. Nieken, in: Abluftreinigung in katalytischen Festbettreaktoren bei periodischer Strömungsumkehr, VDI-Fortschrittberichte, VDI-Verlag, Düsseldorf, 1993.
[38] U. Nieken, G. Eigenberger, Catalytic combustion with periodic flow reversal, Chem. Eng. Sci. 43 (1988) 2109–2115.
[39] H. Klein, in: Untersuchungen zum Betriebsverhalten eines Thermokompressors, VDI-Fortschrittberichte,VDI-Verlag, Düsseldorf, 1996.
[40] A. Spieth, MAPLE V Release 2, Referenzhandbuch, Thompson Publishing GmbH, 1994.
[41] S.V. Patankar, in: Numerical Heat Transfer and Fluid Flow, Hemisphere, Washington, DC, 1980.
[42] P. Deuflhard, E. Hairer, J. Zugk, One-step and extrapolation methods for differential–algebraic systems, Numer. Math. 51 (1987) 501–516.